UC Irvine
UC Irvine Previously Published Works

Title

Ultrahigh-resolution optical coherence tomography by broadband continuum generation from a photonic crystal fiber.

Permalink

Journal

ISSN

Authors

Wang, Yimin
Zhao, Yonghua
Nelson, JS
et al.

Publication Date

DOI

Copyright Information

Peer reviewed

Ultrahigh-resolution optical coherence tomography by broadband continuum generation from a photonic crystal fiber

Yimin Wang, Yonghua Zhao, J. S. Nelson, and Zhongping Chen

Beckman Laser Institute and Department of Biomedical Engineering, University of California, Irvine, Irvine, California 92612

Robert S. Windeler

Bell Laboratories, Lucent Technologies, Murray Hill, New Jersey 70974

We have developed an ultrahigh-resolution optical coherence tomographic system in which broadband continuum generation from a photonic crystal fiber is used to produce high longitudinal resolution. Longitudinal resolution of 1.3-μm has been achieved in a biological tissue by use of continuum light from 800 to 1400 nm. The system employed a dynamic-focusing tracking method to maintain high lateral resolution over a large imaging depth. Subcellular imaging is demonstrated. © 2003 Optical Society of America

OCIS code: 170.4500.

Optical coherence tomography (OCT) can be used for *in vivo* high-resolution cross-sectional imaging of biological tissues.[1–3] Longitudinal resolution, governed by source coherence length, is inversely proportional to the light source's bandwidth. Superluminescent diodes (SLDs) are often used for OCT imaging and typically have 10–15-μm longitudinal resolution.[4] However, the limited optical bandwidth of SLDs precludes imaging on a cellular level. In addition, achieving faster imaging speed with a high signal-to-noise ratio requires more than the milliwatt-level power that is typically available from SLD sources. A Kerr-lens mode-locked Ti:sapphire laser, optimized for a short coherence length, has achieved sub-2-μm longitudinal resolution.[5] Although this source provided cellular resolution imaging, comparative studies have shown that the 0.8-μm center wavelength of the Ti:sapphire laser is not optimal for deep penetration into highly scattering biological tissues. Ultrahigh-resolution OCT imaging in the spectral region from 1.1 to 1.5 μm requires extremely broad bandwidths because of the $\lambda^2/\Delta\lambda$ dependence of the longitudinal resolution. However, this spectral region is of particular interest for OCT because it penetrates deeply into biological tissue and permits spectrally resolved imaging of water absorption bands. *In vivo*, OCT imaging with 5.1-μm longitudinal resolution at 1300 nm was demonstrated with a Kerr-lens mode-locked solid-state laser.[6] However, the improvement in resolution is constrained by the limited output bandwidth of the laser.

Highly-nonlinear air–silica microstructure fibers and photonic crystal fibers (PCFs) can generate an extremely broadband continuum light spectrum from the visible to the near infrared by use of low-energy femtosecond pulses.[7] This spectrum is achieved because of the waveguide dispersion characteristics of the fibers, which shift the zero-dispersion wavelength to shorter wavelengths, and the small core diameters, which provide tight mode confinement. An OCT system with a longitudinal resolution of 2.5 μm with

a PCF source at a wavelength of 1.3 μm has been reported.[8] However, the system has a limited depth range because no dynamic focus tracking is implemented. In this Letter we describe the application of a PCF source for ultrahigh-resolution OCT imaging. In our experiment, 1.3-μm longitudinal resolution was achieved in tissue with a center wavelength of 1.1 μm. To our knowledge, this is the highest resolution reported for this wavelength range. The system also incorporated a dynamic focus tracking method that significantly increased the depth range of ultrahigh-resolution imaging. Subcellular imaging over a large depth range has been demonstrated.

Fiber-based systems have been widely used in OCT. However, several limitations become apparent when a fiber-based OCT system is used for high-resolution imaging. First, it is difficult to construct a 2 × 2 coupler with a bandwidth of more than 200 nm. Second, because of chromatic aberration, a lens system with fiber collimators or focusing elements will limit the efficient bandwidth. Third, the fiber would be multimode if the short-wavelength limit of the spectrum were shorter than the cutoff wavelength of the fiber. The multiple modes will introduce ghost lines into the OCT image. Finally, polarization mode dispersion in a single-mode fiber may also limit longitudinal resolution. To overcome these limitations, we designed and constructed an open-air ultrahigh-resolution OCT system, as shown in Fig. 1. To achieve high lateral resolution it is necessary to use an objective lens with a high numerical aperture to obtain a small focusing size. However, a small focusing size also means a small confocal parameter, which is connected with the longitudinal imaging range. To get deep longitudinal imaging while maintaining constant high lateral resolution, several methods were developed to overcome that problem. One example is the use of C-mode scanning to reconstruct tomographic images, but this increases image acquisition time. In our system, an objective lens and a rectangular prism are both
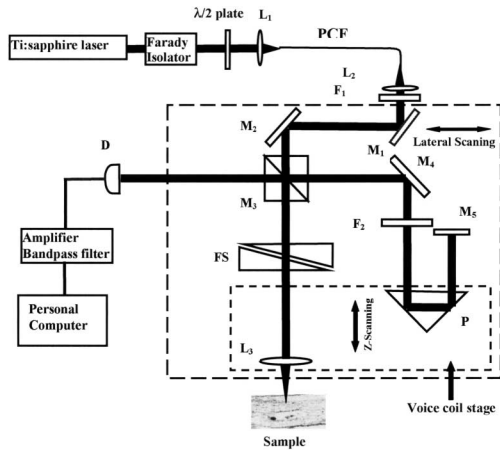
Fig. 1. Schematic of the ultrahigh-resolution OCT system: M_3, wideband cube beam splitter; M_1, M_2, M_4, M_5, silver mirrors; F_1, long-pass filter; L_1, coupling lens; L_2, collimated lens; L_3, objective lens; P, rectangular prism; D, InGaAs detector; F_2, is a neutral-density filter; PCF, photonic crystal fiber; FS, fused-silica prisms.

mounted upon a voice-coil translation stage to track dynamic focusing during longitudinal scanning.[9] This makes it possible to increase imaging depth with constant high lateral resolution. The baseplate is mounted upon a stage for lateral scanning.

The interferometer's light source is broadband continuum generation from a PCF, as shown in Fig. 1. The pump source for the PCF was a Kerr-lens mode-locked Ti:sapphire laser. The total output laser power was greater than 700 mW, with a pulse duration of 110 fs and a repetition rate of 76 MHz. The laser output wavelength was 780 nm. The laser beam was then coupled into the PCF after a Faraday isolator to prevent interference of backreflected light with the mode locking and the $\lambda/2$ wave plate, as shown in Fig. 1. The focal length of the coupling lens was 6.5 mm. Nitrogen gas was slowly blown onto the coupling part to purge the fiber tip and prevent damage. A $\lambda/2$ wave plate after the Faraday isolator was used to adjust the polarization state of the light input to the fiber to optimize the spectrum. The spectrum of light was broadened as it propagated through the fiber because of self-phase modulation and Raman scattering. The continuum output of light was collimated by a 4.5-mm focal-length lens, L_2. Continuum light generation from 400 to 1400 nm was observed from the fiber. The output spectrum after passing through an 800-nm long-pass filter is shown in Fig. 2(a). The spectrum ranged from 800 to 1430 nm. The total output power from the PCF could be as high as 100 mW, and the remaining power was approximately 50 mW after a long-pass filter.

To achieve ultranarrow-field correlation it is important to balance the group-velocity dispersion (GVD) of the two arms of the interferometer. For a light source with a Gaussian spectrum, the width of the field autocorrelation function increases according to[10]

$$\sigma_t = \sigma_{t0}\left\{1 + \left[\frac{\mathrm{d}^2\phi(\omega)}{\mathrm{d}\omega^2}\right]^2 \sigma_\omega^4\right\}^{1/2}, \qquad (1)$$

where σ_t is the $1/e^{1/2}$ half-width of the autocorrelation function, σ_{t0} is the zero-dispersion width of the autocorrelation function, and σ_w is the $1/e^{1/2}$ half-width of the spectrum. The equation shows that the larger the source bandwidth, the more sensitive to GVD the measurement is. For this reason, we chose a pair of prisms made from fused silica to balance the system GVD and used two SLD sources, with wavelengths of 650 and 950 nm. When GVD in the system was not compensated for, the fringes of 650 and 950 nm were separated from each other. Through adjustment of the prism, the distance between these fringes could be eliminated. When the GVD was balanced, the two fringes perfectly overlapped. Thus, with this method, the GVD in the system could be accurately balanced. In the experiment the ultrahigh-resolution OCT system was optimized to support 1.8-μm longitudinal resolution in free space at a center wavelength of 1.1 μm. Figure 2(b) shows the interference fringe with a silver mirror as the sample. The envelope is shown in Fig. 2(d), and it can be seen that the longitudinal resolution is 1.8 μm. Considering the refractive index of tissue, the corresponding resolution is 1.3 μm in tissue. Because the spectrum from the PCF is not perfectly Gaussian shaped, sidelobes in the interferometric autocorrelation are visible. The detected optical spectrum is shown in Fig. 2(c), which was calculated by Fourier transformation of the interferometric signal shown in Fig. 2(b). The detected spectral bandwidth is reduced to 372 nm at a center wavelength of 1.1 μm. This reduction of the bandwidth occurs in the short-wavelength part of the spectrum and is caused by the low sensitivity of our detector at wavelengths shorter than 0.9 μm.

The lateral resolution of the system was 4 μm, which was determined by the achromatic lens. The improvement in axial resolution was demonstrated in the following experiment: A plastic film of 21-μm thickness was chosen as the sample. Two glass plates were used to clip the film. Index-matching oil was put onto the upper and lower sides of the film to reduce reflection. The power of the light to the system was 50 mW. The OCT image is shown in Fig. 3. The image size was 0.75 mm $\times$ 0.15 mm at $\sim$1.8 μm $\times$ 4 μm (longitudinal $\times$ lateral) resolution. Note that the
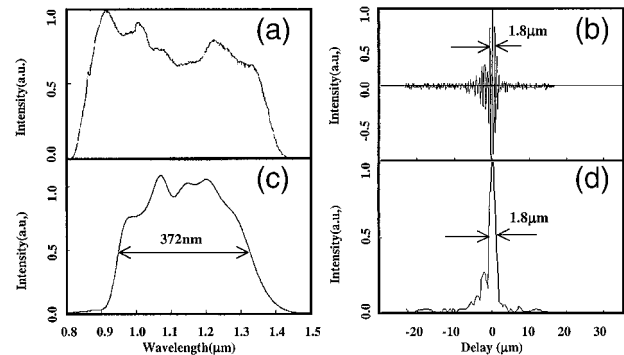

Fig. 2. (a) Spectrum of the light source from the crystal fiber after a long-pass filter, (b) interference signal at the photodetector, (c) spectrum calculated by Fourier transformation, (d) interference envelope of the signal shown in (b).
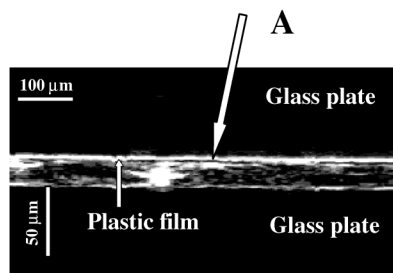
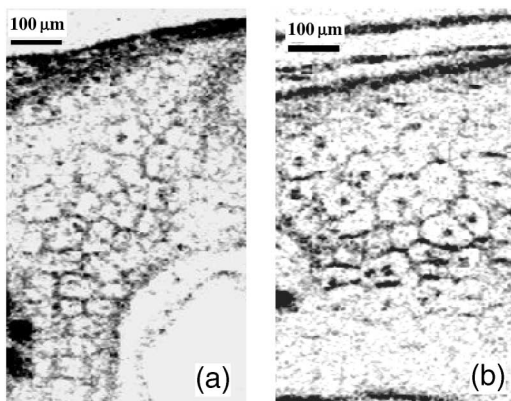Fig. 3. OCT image with a 21-μm-thick plastic film sample.

Fig. 4. (a) OCT image of a tadpole for which the dynamic focusing technique was used. Image size, 0.5 mm × 1.0 mm. (b) OCT image of the tadpole without dynamic focusing. Image size, 0.5 mm × 1.0 mm.

structure inside the film can be observed. In particular, the gap between the glass plate and upper surface of the film can be clearly seen. Compared with the 21-μm film thickness, the calibrated thickness of the gap at A is 2 μm. Thus, with broadband continuum light from a PCF source, OCT axial resolution has been significantly improved.

The feasibility of *in vivo* ultrahigh-resolution imaging was demonstrated with an animal model, a *Xenopus* tadpole. Figure 4(a) shows an *in vivo* OCT image of a 35-day-old anesthetized specimen. The tadpole was placed in tank water in a dish to prevent dehydration and to provide index matching. The incident power to the system was 50 mW. The voice coil stage was scanned at a speed of 4 mm/s at a repetition rate of 1 Hz. Figure 4(a) shows an area of 0.5 mm × 1.0 mm imaged at 1.3 μm × 4 μm (longitudinal × lateral) resolution. Membranes and nuclei can be clearly seen, and single-cell structure can be identified in the image.

To demonstrate the advantage of dynamic focusing for improved imaging depth while maintaining high lateral resolution, another experiment was performed. Here a normal interference structure without dynamic focusing was constructed. The OCT image of a 21-day-old specimen is shown in Fig. 4(b). The resolution in Fig. 4(b) is 1.3 μm × 4 μm

(longitudinal × lateral). Single cells can be seen, but the imaging depth is greatly reduced compared with that of the image obtained by the dynamic-focusing technique. Because of the high lateral resolution, the confocal parameter of our objective lens was only 33.8 μm in air, which resulted in image degradation outside the focused zone. Thus, dynamic focusing has been employed successfully in ultrahigh-resolution OCT imaging.

In summary, we have demonstrated an ultrahigh-resolution optical coherence tomography system that uses broadband-continuum generation from a photonic crystal fiber as the light source. We achieved a longitudinal resolution of 1.8 μm in air (~1.3 μm in tissue) at a center wavelength of 1.1 μm. The broad bandwidth of the light source permits both high-resolution and spectroscopic OCT imaging in wavelength ranges that were previously not accessible. The system is capable of dynamic focusing compensation to maintain constant lateral resolution for large imaging depth.

References

1. D. Huang, E. Swanson, C. P. Lin, J. S. Schuman, W. G. Stinson, W. Chang, M. R. Hee, T. Flotte, K. Gregory, C. A. Puliafito, and J. G. Fujimoto, Science **254**, 1178 (1991).
2. J. M. Schmitt, S. L. Lee, and K. M. Yung, Opt. Commun. **142**, 203 (1997).
3. J. G. Fujimoto, M. E. Brezinski, G. J. Tearney, S. A. Boppart, B. E. Bouma, M. R. Hee, J. F. Southern, and E. A. Swanson, Nature Med. **1**, 970 (1995).
4. R. C. Youngquist, S. Carr, and D. E. N. Davies, Opt. Lett. **12**, 158 (1987).
5. W. Drexler, U. Morgner, F. X. Kärtner, C. Pitris, S. A. Boppart, X. D. Li, E. P. Ippen, and J. G. Fujimoto, Opt. Lett. **24**, 1221 (1999).
6. S. A. Boppart, B. E. Bouma, C. Pitris, J. F. Southern, M. E. Brezinski, and J. G. Fujimoto, Nature Med. **4**, 861 (1998).
7. J. K. Ranka, R. S. Windeler, and A. J. Stentz, Opt. Lett. **25**, 25 (2000).
8. I. Hartl, X. D. Li, C. Chudoba, R. K. Ghanta, T. H. Ko, and J. G. Fujimoto, Opt. Lett. **26**, 608 (2001).
9. Z. Chen, T. E. Milner, D. Dave, and J. S. Nelson, Opt. Lett. **22**, 64 (1997).
10. B. L. Danielson and C. Y. Boisrobert, Appl. Opt. **30**, 2975 (1991).